

See discussions, stats, and author profiles for this publication at: <https://www.researchgate.net/publication/263208480>

# DFT study on the reaction mechanisms and stereoselectivities of NHC-catalyzed [2+2] cycloaddition between arylalkylketenes and electron-deficient benzaldehydes

ARTICLE *in* ORGANIC & BIOMOLECULAR CHEMISTRY · JUNE 2014

Impact Factor: 3.56 · DOI: 10.1039/c4ob00606b · Source: PubMed

---

CITATIONS

5

---

READS

24

## 7 AUTHORS, INCLUDING:



Donghui Wei

Zhengzhou University

65 PUBLICATIONS 506 CITATIONS

[SEE PROFILE](#)



Yanyan Zhu

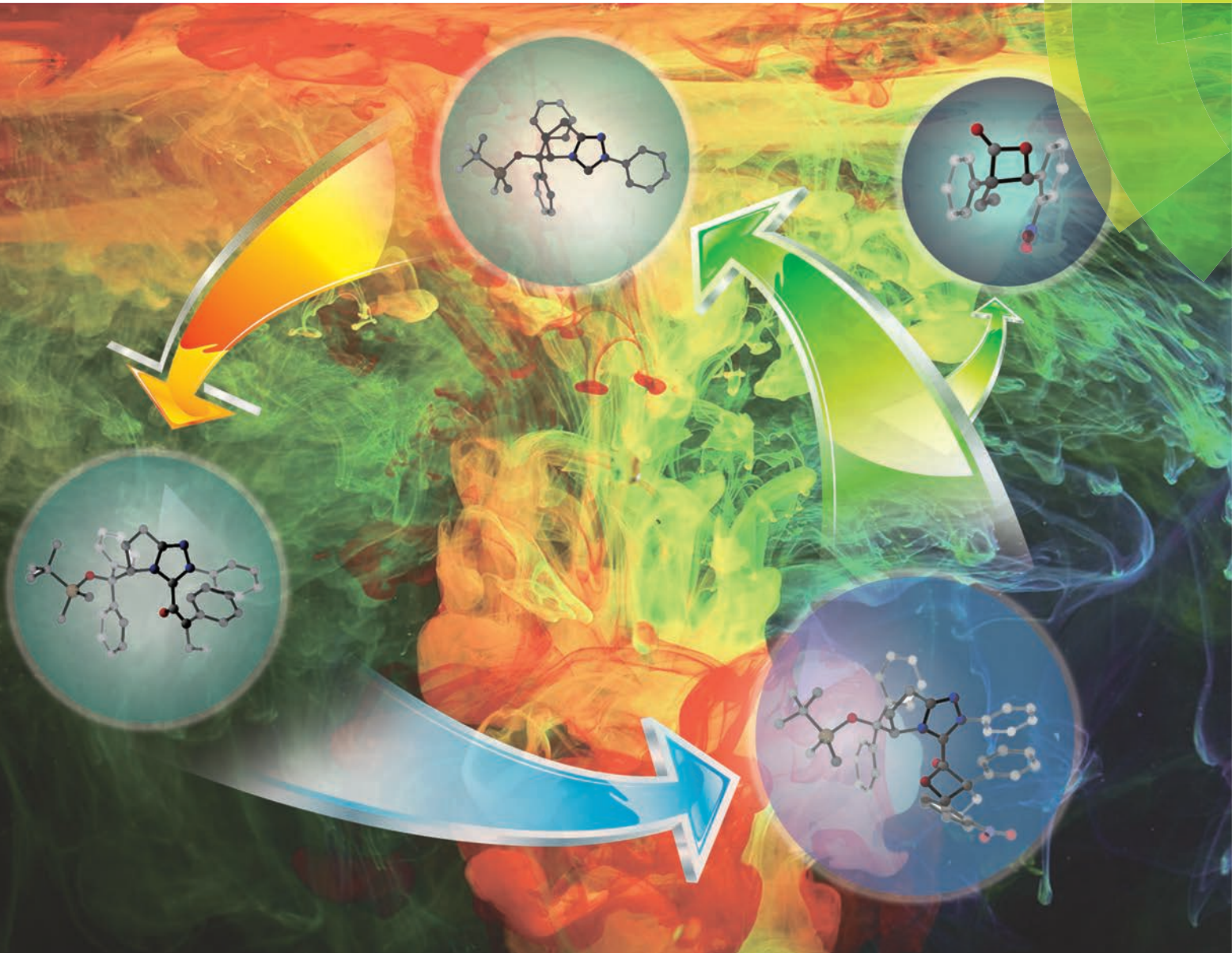
Zhengzhou University

55 PUBLICATIONS 606 CITATIONS

[SEE PROFILE](#)

# Organic & Biomolecular Chemistry

[www.rsc.org/obc](http://www.rsc.org/obc)



ISSN 1477-0520



PAPER

Donghui Wei, Yanyan Zhu *et al.*  
DFT study on the reaction mechanisms and stereoselectivities of NHC-catalyzed [2 + 2] cycloaddition between arylalkylketenes and electron-deficient benzaldehydes



Cite this: *Org. Biomol. Chem.*, 2014,  
12, 6374

## DFT study on the reaction mechanisms and stereoselectivities of NHC-catalyzed [2 + 2] cycloaddition between arylalkylketenes and electron-deficient benzaldehydes†

Mengmeng Zhang, Donghui Wei,\* Yang Wang, Suiji Li, Jiefei Liu, Yanyan Zhu\* and Mingsheng Tang

In this paper, two possible mechanisms (mechanisms A and B) on the stereoselective [2 + 2] cycloaddition of aryl(alkyl)ketenes and electron-deficient benzaldehydes catalyzed by N-heterocyclic carbenes (NHCs) have been investigated using density functional theory (DFT). Our calculated results indicate that the favorable mechanism (mechanism A) includes three processes: the first step is the nucleophilic attack on the arylalkylketene by the NHC catalyst to form an intermediate, the second step is the [2 + 2] cycloaddition of the intermediate and benzaldehyde for the formation of a  $\beta$ -lactone, and the last step is the dissociation of the NHC catalyst and the  $\beta$ -lactone. Notably, the [2 + 2] cycloaddition, in which two chiral centers associated with four configurations (*SS*, *RR*, *SR* and *RS*) are formed, is demonstrated to be both the rate- and stereoselectivity-determining step. Moreover, the reaction pathway associated with the *SR* configuration is the most favorable pathway and leads to the main product, which is in good agreement with the experimental results. Furthermore, the analysis of global and local reactivity indexes has been performed to explain the role of the NHC catalyst in the [2 + 2] cycloaddition reaction. Therefore, this study will be of great use for the rational design of more efficient catalysts for this kind of cycloaddition.

Received 21st March 2014,  
Accepted 13th May 2014

DOI: 10.1039/c4ob00606b  
[www.rsc.org/obc](http://www.rsc.org/obc)

## 1. Introduction

As a versatile starting material for complex molecule, building block synthesis, and a monomer in biodegradable polymer synthesis,<sup>1</sup> as well as being the core structure in a range of natural products with notable pharmacological properties, the  $\beta$ -lactone motif has attracted more and more attention in chemistry.<sup>2</sup>  $\beta$ -Lactones, which are synthesized in large quantities experimentally, serve as useful intermediates in an array of fields, including materials science and synthetic organic chemistry.

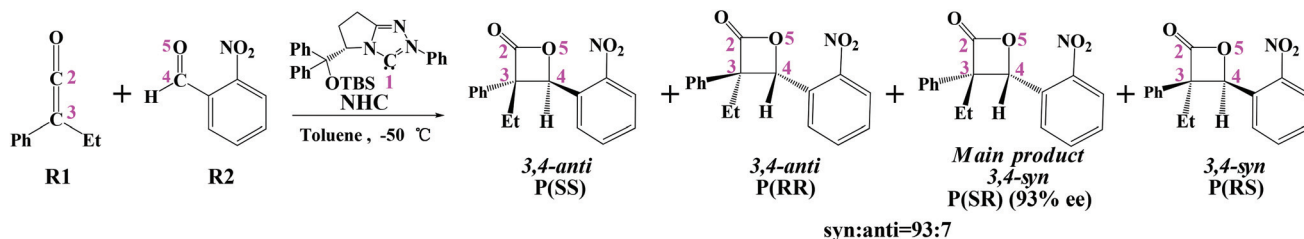
Generally,  $\beta$ -lactones can be obtained by ketene and aldehyde (or ketone) [2 + 2] cycloaddition reactions.<sup>3</sup> The direct [2 + 2] cycloaddition of carbonyl compounds and ketenes has been known since 1911,<sup>3b</sup> and great efforts have been made towards the development of the synthesis of  $\beta$ -lactones in experiments over the following hundred years.<sup>2a</sup> Notably, Lewis acid catalysis is a very convenient method and has been

widely used in ketene and aldehyde (or ketone) [2 + 2] cycloadditions.<sup>2b,4</sup> However, most of these reactions have very poor stereoselectivity. In 1995, Yamamoto and co-workers utilized a highly efficient Lewis acid catalyst for achieving high stereoselectivity in the cycloaddition of trialkylsilylketene with aldehydes.<sup>5</sup> In addition, NHC-catalyzed ketene cycloaddition reactions have been reported as an effective and high stereoselective route to form  $\beta$ -lactones in recent years.<sup>6</sup> For example, Smith *et al.* reported that the [2 + 2] cycloaddition reactions of arylalkylketenes and electron-deficient benzaldehydes catalyzed by NHC can generate  $\beta$ -lactones in high yield and stereoselectivity (Scheme 1).<sup>1b</sup>

Due to the special reactivity and wide applications of ketene and aldehyde (or ketone) [2 + 2] cycloadditions in organic chemistry, their theoretical study has also attracted more and more attention. In addition, there have been several theoretical studies on the reaction mechanisms of ketene and aldehyde (or ketone) [2 + 2] cycloadditions under non-catalyzed and Lewis acid-catalyzed conditions.<sup>7</sup> For example, Cossio and co-workers studied the possible reaction paths corresponding to Lewis acid-catalyzed and uncatalyzed reactions between chloroketene (as a model activated ketene) and acetaldehyde (as a model alkyl carbonyl compound) using *ab initio* methodologies and taking into account solvent effects.<sup>7c</sup> Rajzmann and

The College of Chemistry and Molecular Engineering, Center of Computational Chemistry, Zhengzhou University, Zhengzhou, Henan Province 450001, P.R. China.  
E-mail: [donghuiwei@zzu.edu.cn](mailto:donghuiwei@zzu.edu.cn), [zhuyan@zzu.edu.cn](mailto:zhuyan@zzu.edu.cn)

† Electronic supplementary information (ESI) available. See DOI: 10.1039/c4ob00606b



Scheme 1 The ketene and benzaldehyde [2 + 2] cycloaddition catalyzed by NHC.

co-authors used semiempirical (AM1/RHF and AM1/CI) and *ab initio* (HF/6-31G\* and MP2/6-31G\*) calculations to study the formation of  $\beta$ -lactone through Lewis acid ( $\text{BH}_3$  and  $\text{BF}_3$ ) promoted ketene–ketone [2 + 2] cycloaddition.<sup>7e</sup> Notably, Yamabe *et al.* provided precise frontier molecular orbital (FMO) pictures for the ketene and aldehyde [2 + 2] cycloadditions under non-catalyzed conditions by tracking the intrinsic reaction coordinate (IRC), and confirmed the FMOs participated in the ketene [2 + 2] cycloaddition reactions.<sup>7d</sup> Furthermore, our previous work investigated the mechanisms of Lewis acid  $\text{BF}_3$ -catalyzed ketene–ketone [2 + 2 + 2] cycloaddition reactions at the B3LYP/6-31G(d,p) level, and we have also explored the frontier molecular orbital (FMO) overlap mode of the ketene–ketone [2 + 2] cycloadditions under  $\text{BF}_3$ -catalyzed conditions.<sup>8</sup>

To the best of our knowledge, no report of theoretical investigations on the mechanism of the Lewis base NHC-catalyzed ketene and aldehyde (or ketone) [2 + 2] cycloaddition reactions has been found up to now. Thus, the reaction mechanisms are still ambiguous, and which step is the stereoselectivity-determining step and which factor is the decisive factor for the stereoselectivity in this kind of reaction remain unclear. In addition, it is essential to make clear why the reaction can occur more easily and has good stereoselectivity under NHC-catalyzed conditions. As described above, we think it is necessary to carry out a detailed mechanistic investigation to complement the experimental study and rationalize the experimental observations. This paper should be helpful for explaining how the NHC catalyst works and what the role of the NHC catalyst is, and will thus be useful for the rational design of potent catalysts for ketene and aldehyde (or ketone) [2 + 2] cycloadditions.

In this project, the [2 + 2] cycloaddition of aryl(alkyl) ketene **R1** and benzaldehyde **R2** promoted by catalyst **NHC** to give the corresponding  $\beta$ -lactone **P(SR)** with 93% ee (Scheme 1) has been chosen as the object of the investigation. As shown in Scheme 1, it should be noted that there are two chiral centers (including C3 and C4 atoms) in the main product **P(SR)**, so we use the two letters in parentheses to represent the chirality of C3 and C4 atoms respectively, and the following suffixes of the stationary points have the same meaning. The reaction mechanisms were studied using density functional theory, which has been widely used in the study of the reaction mechanisms.<sup>9</sup>

## 2. Computational details

All theoretical calculations were performed using the Gaussian 09 program package.<sup>10</sup> Density functional theory (DFT), which has been proved to be a powerful tool for the study of reaction mechanisms, was chosen in this computational work.<sup>11,12</sup> Considering the complexity of the theoretical model used for this study, all the structural optimizations were carried out at the M06-2X<sup>13</sup>/6-31G(d,p) level in toluene solvent, using the integral equation formalism polarizable continuum model (IEF-PCM).<sup>14</sup> Additionally, the structures (local minima or first-order saddle points) were located by performing full geometry optimization without any symmetric restriction. Then the corresponding vibrational frequencies were calculated at the same level to take account of the zero-point vibrational energy (ZPVE) and to identify the transition states. We confirmed that all the reactants, reaction precursors, intermediates, and products have no imaginary frequencies, and each transition state has one, and only one, imaginary frequency. Intrinsic reaction coordinate (IRC) calculations<sup>15</sup> at the same level were performed to verify that each saddle point links two desired minima and the transition states led to the expected reactants and products.

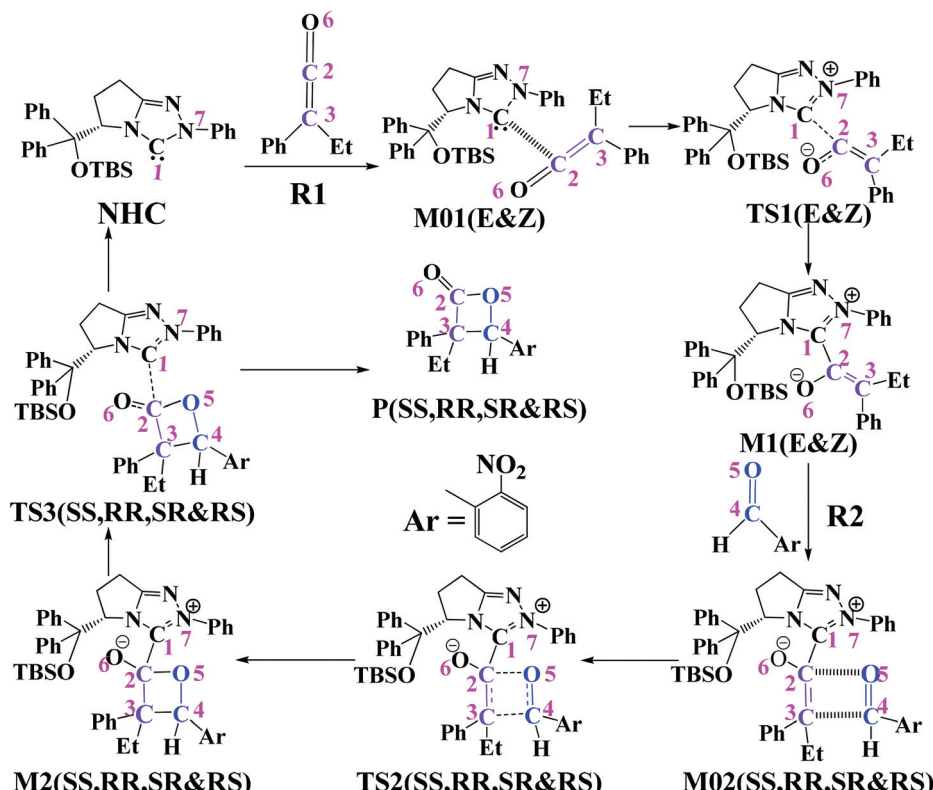
Based on the optimized structures, the single-point energies were further refined using the 6-311+G(d,p) basis set in toluene solvent. All discussions in this paper are based on the Gibbs free energies.

## 3. Results and discussion

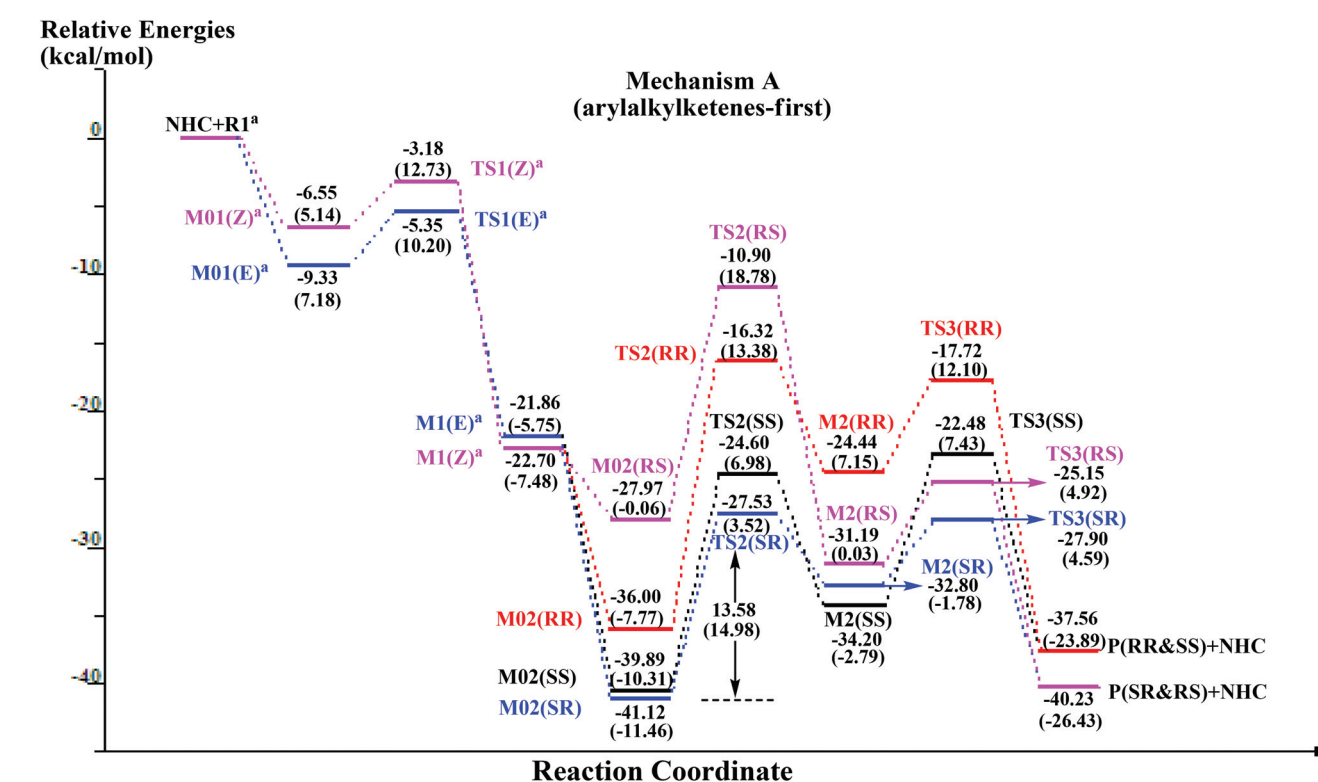
### 3.1. Reaction mechanisms of the title reaction

**3.1.1. Mechanism A.** Firstly, we have suggested the possible catalytic mechanism A for the title reaction, which is depicted in Scheme 2. As shown in Scheme 2, there are three steps involved in mechanism A: the complexation of **NHC** and **R1**, the [2 + 2] cycloaddition, and the regeneration of catalyst **NHC**. The corresponding energy profile for mechanism A is depicted in Fig. 1. As shown in Fig. 1, we set the Gibbs free energies of **R1** + **R2** + **NHC** as 0.00 kcal mol<sup>-1</sup> as references in the energy profile.

The first step of the reaction in mechanism A is the combination of **NHC** with **R1**. **M01(E)** and **M01(Z)** (Fig. 2) are the reaction precursors, which are formed by the weak interactions



Scheme 2 The possible reaction mechanism A.

Fig. 1 Energy ( $E + ZPVE$ ) profile of the possible reaction mechanism A. Numbers in parentheses are relative Gibbs free energies (unit: kcal mol<sup>-1</sup>; the superscript "a" represents adding the energy of R2).

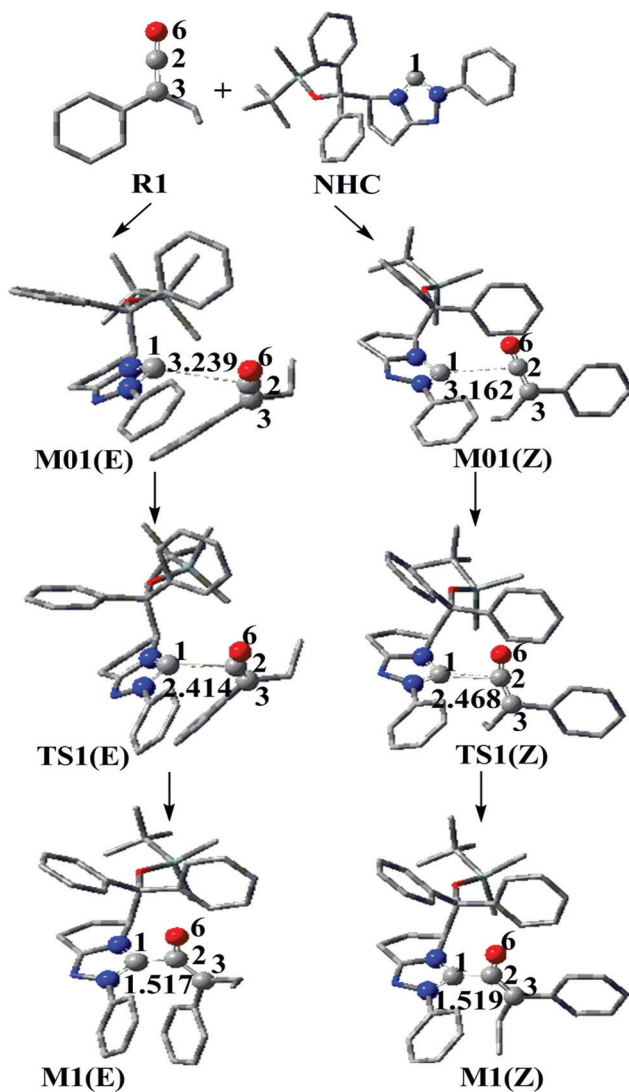


Fig. 2 Optimized structures of the reactants (NHC and R1), the reaction precursors M01(E&Z), transition states TS1(E&Z), and intermediates M1(E&Z) (distances in Å).

between NHC and R1. For the double bond C<sub>2</sub>=C<sub>3</sub>, M1(E) and M1(Z) are a pair of *E* and *Z*-isomers. In this step, the approach of NHC to the ketene would lead to the intermediates M1(E&Z) via transition states TS1(E&Z). The distance of C<sub>1</sub>-C<sub>2</sub> is 2.414 Å in TS1(E) and 2.468 Å in TS1(Z), which are shortened to 1.517 Å in M1(E) and 1.519 Å in M1(Z) (Fig. 2). It is clear that a single bond is already formed between the C<sub>1</sub> atom and the C<sub>2</sub> atom in M1(E&Z).

As can be seen from Table 1, the values of NBO charge on the C<sub>1</sub> and C<sub>2</sub> atoms change drastically from 0.135e in NHC and 0.744e in R1 to ~0.49e and ~0.35e in M1(E&Z) respectively, demonstrating that the charge transferred from NHC to R1 in this process. Apart from the above, the charge value of the N<sub>6</sub> atom changes from -0.266e in NHC to -0.180e in M1(E) (-0.182e in M1(Z)), at the same time, the charge value of O<sub>6</sub> atom changes from -0.454e in R1 to -0.746e in M1(E) (-0.741 e

Table 1 The values of NBO charge on the C<sub>1</sub>, C<sub>2</sub>, O<sub>6</sub>, and N<sub>7</sub> atoms in R1, NHC, M1(E), and M1(Z) at the M06-2X/6-31G (d,p) level (unit: e)

	C1	C2	C3	O6	N7
R1	—	0.744	-0.335	-0.454	—
NHC	0.135	—	—	—	-0.266
M1(E)	0.496	0.345	-0.210	-0.746	-0.180
M1(Z)	0.492	0.345	-0.208	-0.741	-0.182

in M1(Z)). Obviously, there is a charge transfer process from catalyst NHC to reactant R1 in this step, which indicates the catalyst NHC should be the Lewis base organocatalyst. The energy barriers of the first step are 3.02 kcal mol<sup>-1</sup> (associated with *E*-configuration TS1(E), Fig. 1) and 7.59 kcal mol<sup>-1</sup> (associated with *Z*-configuration TS1(Z), Fig. 1). Moreover, M1(E) lies 5.75 kcal mol<sup>-1</sup> below the energy of the reactants, while M1(Z) lies 7.48 kcal mol<sup>-1</sup> below the energies of the reactants.

The second step in mechanism A is the formation of four-membered ring (C<sub>2</sub>-C<sub>3</sub>-C<sub>4</sub>-O<sub>5</sub>) through [2 + 2] cycloaddition. In this step, the reaction precursor M02(SS,RR,SR&RS) could become the intermediate M2(SS,RR,SR&RS) via the four-membered ring transition state TS2(SS,RR,SR&RS) (see Fig. 3 and Fig. S1–S3 in ESI†). Scheme 3 illustrates the stereochemistry of this step (the *Si* or *Re* face of M1 is in terms of the prochiral atom C<sub>3</sub>, and the *Si* or *Re* face of R2 is in terms of the prochiral atom C<sub>4</sub>). Attacking from the *Re* face of M1 on the *Re* or *Si* face of R2 can lead to intermediate M2(SS) or M2(SR), separately. Similarly, the *Si* face attack of M1 can only lead to the *R* configuration of C<sub>3</sub>. That is to say, the attack from the *Si* face of M1 on the *Re* or *Si* face of R2 can only lead to intermediate M2(RS) or M2(RR), respectively. Therefore, there are four different kinds of stereoisomer, *i.e.* SS, SR, RS, and RR configurations, in this [2 + 2] cycloaddition process. Accompanied with the

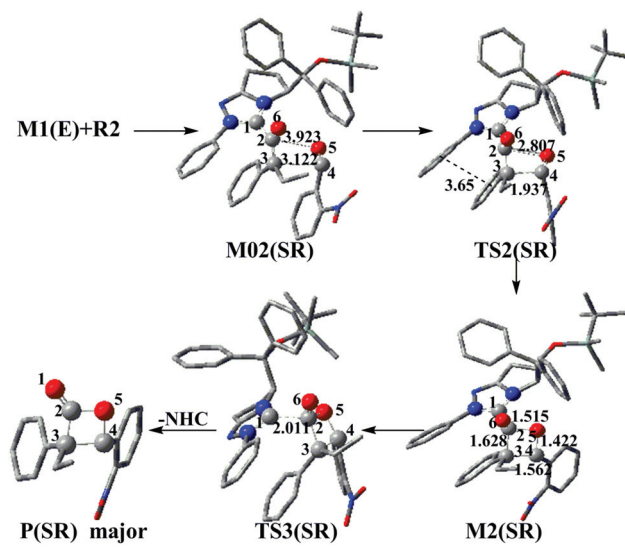
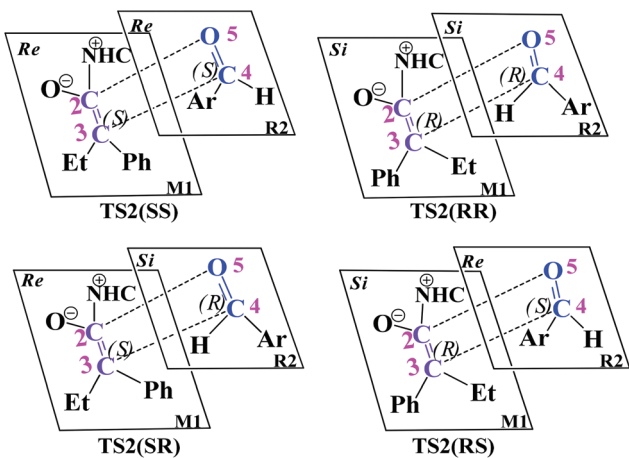


Fig. 3 Optimized structures for M02(SR), TS2(SR), M2(SR), TS3(SR), and P(SR) (distances in Å).



Scheme 3 The four attack modes of M1 to R2 via TS2(SS,RR,SR&RS).

formation of bond C3–C4, the single bond C2–O5 is also generated subsequently in **M2(SS,RR,SR&RS)** (see Fig. 3 and Fig. S1–S3 in ESI†) via TS2(SS,RR,SR&RS), so the [2 + 2] cycloaddition is a concerted process.

The distances C2–C3, C4–O5, C3–C4, and O5–C2 in **M02(SS,RR,SR&RS)**, TS2(SS,RR,SR&RS) and **M2(SS,RR,SR&RS)** are summarized in Table 2. As can be seen from Table 2, the distances C3–C4 and O5–C2 are shortened, whereas the distances C2–C3 and C4–O5 are lengthened in this process. Finally, the C3–C4 and O5–C2 bonds are formed, and the double bonds C2–C3 and C4–O5 become single bonds in **M2(SS,RR,SR&RS)**, separately.

As depicted in Scheme 3, the different stereoselectivities associated with the chiral carbon centers C3 and C4 are generated in the [2 + 2] cycloaddition process, so we think the second step should be the key for the stereoselectivity. As shown in Fig. 2, the energy barrier via TS2(SS,RR,SR&RS) is 17.29/21.15/14.98/18.84 kcal mol<sup>-1</sup>, indicating the pathway associated with TS2(SR) has the lowest energy barrier among the four competing pathways, thus, it should be the most favorable pathway and the SR configuration would be the favorable stereoisomer; this is in agreement with the experiment. In addition, the difference of the energy barrier between SR and RS

Table 2 Some geometrical parameters of several stationary points (SP) along the reaction coordinate (distances in Å)

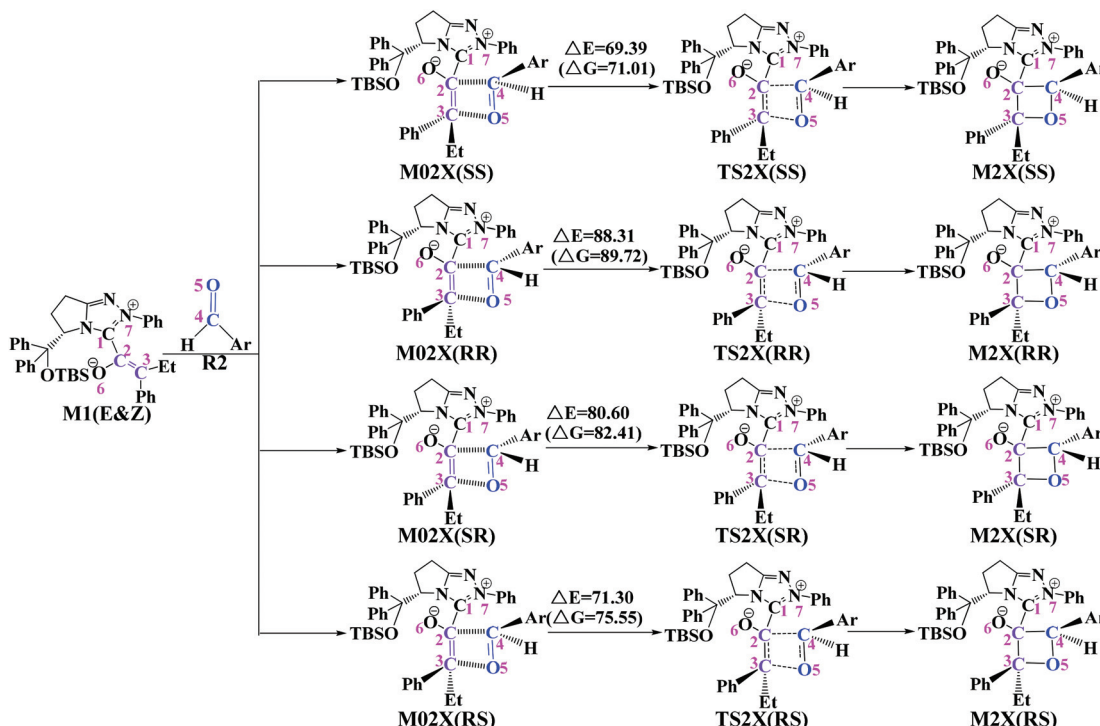
SP	C2–C3	C4–O5	C3–C4	O5–C2
<b>M02(SS)</b>	1.380	1.217	3.270	3.931
<b>M02(RR)</b>	1.388	1.215	3.150	4.215
<b>M02(SR)</b>	1.385	1.216	3.122	3.923
<b>M02(RS)</b>	1.388	1.215	3.030	3.023
<b>TS2(SS)</b>	1.471	1.283	1.977	2.643
<b>TS2(RR)</b>	1.474	1.286	1.895	2.807
<b>TS2(SR)</b>	1.459	1.285	1.937	2.807
<b>TS2(RS)</b>	1.479	1.297	1.864	2.504
<b>M2(SS)</b>	1.638	1.416	1.564	1.553
<b>M2(RR)</b>	1.619	1.423	1.566	1.489
<b>M2(SR)</b>	1.628	1.422	1.562	1.515
<b>M2(RS)</b>	1.612	1.419	1.561	1.497

configurations in this step is 3.86 kcal mol<sup>-1</sup>; this value corresponds to an enantiomeric excess of 99%,<sup>9d,16</sup> which is close to the experimental outcome (93% ee). It should be noted that the benzene ring of the ketene and the phenyl group of the catalyst are parallel stacking, and the distance between them is 3.65 Å in **TS2(SR)**. Therefore, there should be a π–π weak interaction, which would be helpful for the stability of the SR configuration and would lead to its stereochemical preference.

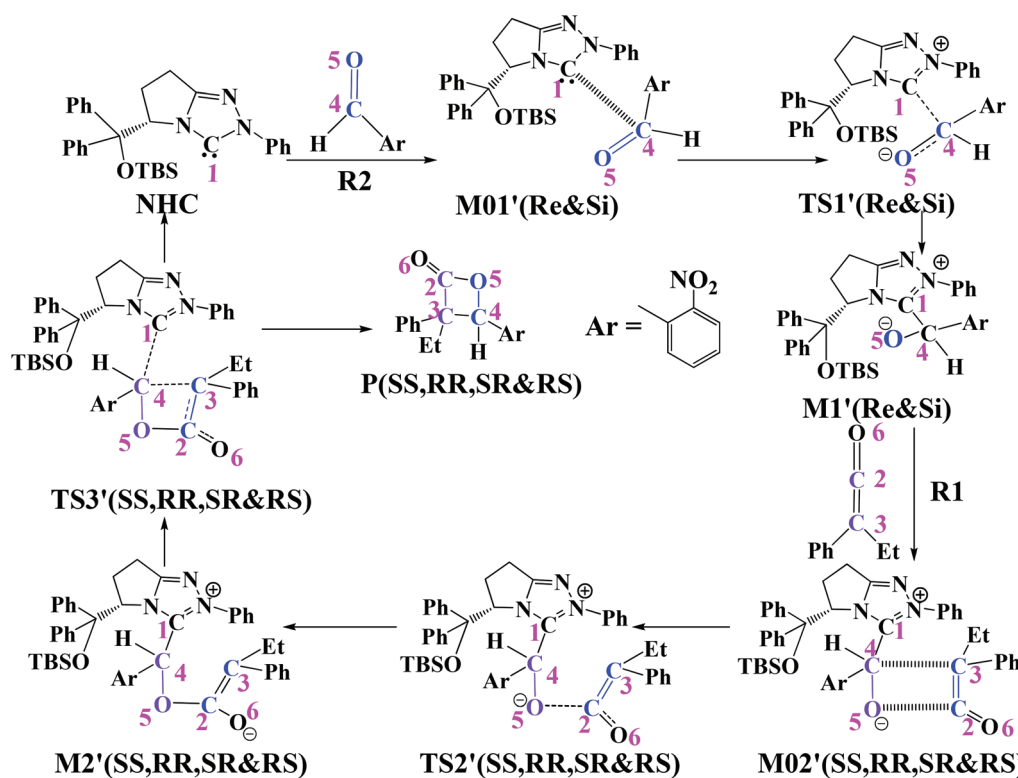
In addition, we have considered the possibility for the stepwise mechanism of the ketene [2 + 2] cycloadditions mentioned in the previous reports.<sup>8,17</sup> We have tried many times to optimize the possible structures of stepwise transition states and intermediates for the [2 + 2] cycloaddition, but we have failed to locate the transition state sand intermediates, so we think the [2 + 2] cycloaddition reaction should be a concerted process. Furthermore, we have investigated another regioisomeric pathway for the [2 + 2] cycloaddition, which is shown in Scheme 4. The energy barriers of the regioisomeric pathways depicted in Scheme 4 are extremely high, so we think the main product should be β-lactone, and this is consistent with the experiment.

In the last step of mechanism A, the catalyst **NHC** and product **P(SS,RR,SR&RS)** would be dissociated by breaking the C1–C2 bond through transition state **TS3(SS,RR,SR&RS)** (see Fig. 3 and Fig. S1–S3 in ESI†), the change of the distance C1–C2 reflects the nature of this reaction process. The distance C1–C2 is lengthened to 2.043/2.045/2.011/2.090 Å in **TS3(SS,RR,SR&RS)**, respectively. The energies of **P(SS,RR,SR&RS)** + **NHC** are 23.89/23.89/26.43/26.43 kcal mol<sup>-1</sup> lower than those of the reactants respectively, indicating the overall reaction is an exothermic process. Furthermore, the energy barrier via **TS3(SS,RR,SR&RS)** is 10.22/4.95/6.73/4.95 kcal mol<sup>-1</sup>, demonstrating that the third step should be a fast process, and the C1–C2 bond in **M2(SS,RR,SR&RS)** will be broken easily under the experimental conditions. Thus, it should be easy for catalyst **NHC** to be released from the entire catalytic cycle.

**3.1.2. Mechanism B.** Notably, the reaction mechanisms and the role of catalyst **NHC** may be different in the different **NHC**-catalyzed ketene cycloadditions,<sup>9c,18</sup> which is due to the different reactants and their special activities. For example, our previous DFT studies have investigated the mechanisms for the enantioselective **NHC**-catalyzed [2 + 2] cycloaddition between aryl(alkyl)ketenes and diazenedicarboxylates, [2 + 2 + 2] cycloaddition between ketenes (two molecules) and carbon disulfide (CS<sub>2</sub>, one molecule), and [4 + 2] cycloaddition between ketenes and *N*-benzoyldiazenes.<sup>9a,c,18</sup> Note that we found that the **NHC** catalysts do not always react with the ketene in the first step of the cycloaddition reaction, which has been discussed in mechanism A. Therefore, we have investigated the possible catalytic mechanism B for the title reaction, which is depicted in Scheme 5. There are three steps involved in mechanism B: the first step is the nucleophilic attack on the carbonyl carbon of **R2** by **NHC** to form a complexation intermediate, the second step is reaction between the intermediate and **R1**, and the last step is S<sub>N</sub>2 nucleophilic substitution to dissociate **NHC** and the product. The



Scheme 4 Another regioisomeric pathway for the [2 + 2] cycloaddition.



Scheme 5 The possible reaction mechanism B.

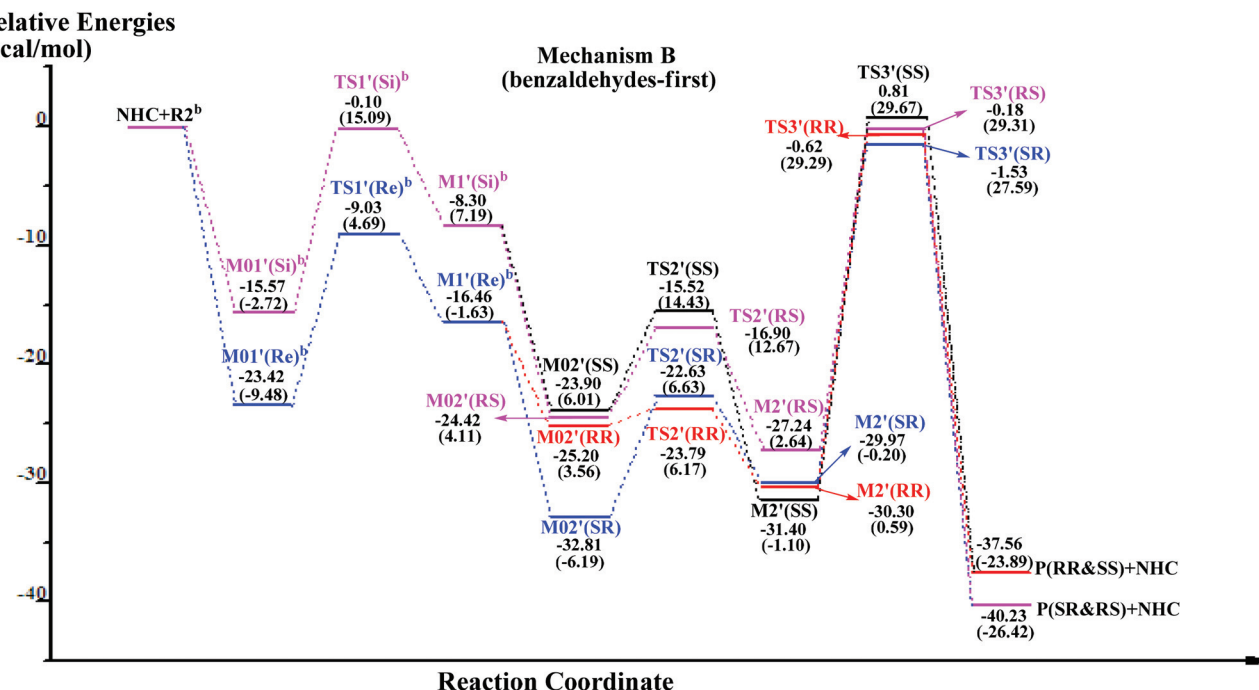


**Fig. 4** Energy ( $E + \text{ZPVE}$ ) profile of the possible reaction mechanism B. Numbers in parentheses are relative Gibbs free energies (unit: kcal mol<sup>-1</sup>; the superscript "b" represents adding the energy of R1).

corresponding energy profile for mechanism B is shown in Fig. 4, we still set the Gibbs free energies of R1 + R2 + NHC as 0.00 kcal mol<sup>-1</sup> as references.

The first step of mechanism B is the combination of NHC with R2, which is remarkably different from mechanism A. In mechanism B, M01'(Re) and M01'(Si) (Fig. 5) are the reaction precursors, which are formed by the weak interactions between NHC and R2. For the prochiral carbon atom (C4), M1'(Re) and M1'(Si) would be associated with the S and R isomers. In this step, NHC nucleophilic attack on benzaldehyde R2 forms the complex M1'(Re&Si) via transition state TS1'(Re&Si) (depicted in Scheme 6). The distance C1–C4 is 2.074 Å in TS1'(Re) and 2.073 Å in TS1'(Si), which is shortened to 1.528 Å in M1'(Re) and 1.517 Å in M1'(Si) (Fig. 5). It is clear that a coordinate bond would be formed between C1 and C4 atoms in M1'(Re&Si).

The second step of mechanism B is the formation of bond C2–O5, and the reaction precursor M02'(SS,RR,SR&RS) transforms to the intermediate M2'(SS,RR,SR&RS) via transition state TS2'(SS,RR,SR&RS) (depicted in Fig. 6 and Fig. S4–S6 in the ESI†). The distances C2–O5 are 2.107/2.137/2.091/2.197 Å in TS2'(SS,RR,SR&RS), which are shortened to 1.459/1.470/1.478/1.466 Å in M2'(SS,RR,SR&RS), indicating the formation of new bond C2–O5 in this step. The energy barrier via TS2'(SS,RR,SR&RS) is 8.42/2.61/12.82/8.56 kcal mol<sup>-1</sup>, demonstrating that the second step should be a fast process, and the C2–O5 bond would be generated easily in M2'(SS,RR,SR&RS) under the experimental conditions.

The last step of mechanism B occurs through a S<sub>N</sub>2 nucleophilic substitution process, *i.e.* the formation of bond C3–C4 is

accompanied with the breaking of bond C1–C2, which leads to the dissociation of catalyst NHC and product (depicted in Fig. 6 and Fig. S4–S6 in the ESI†). This S<sub>N</sub>2 nucleophilic substitution is a concerted process *via* transition state TS3'(SS,RR,SR&RS). The distance between C1 and C2 atoms is 2.036/2.024/1.910/1.987 Å in TS3'(SS,RR,SR&RS), whereas the distance between C3 and C4 atoms is 2.178/2.226/2.192/2.167 Å. The calculated energy barrier *via* TS3'(SS,RR,SR&RS) is 30.77/28.70/27.79/26.67 kcal mol<sup>-1</sup>, which is much higher than those of the first and second steps in mechanism B, therefore, we think the third step should be the rate-determining step. Notably, the energy barrier of the rate-determining step in mechanism B (Fig. 4) is higher than that in mechanism A (Fig. 1), indicating that mechanism B should be not favorable in the competition with mechanism A and cannot really take place in the experiment.

### 3.2. Analysis of the global and local reactivity indexes of the reactants in the [2 + 2] cycloaddition step

As described above, we know that the [2 + 2] cycloaddition in mechanism A should be both the rate-determining and stereo-selectivity-determining step for the title reaction. In order to understand the role of the catalyst NHC in detail, we have also analyzed the global reactivity indexes of the reactants in this key [2 + 2] cycloaddition step. As summarized in Table 3, the molecule global electrophilicity character is measured by the electrophilicity index,  $\omega$ ,<sup>19</sup> which is obtained from the following expression,  $\omega = (\mu^2/2\eta)$ ,<sup>19,20</sup> in terms of the electronic chemical potential  $\mu$  and the chemical hardness  $\eta$ . Both quantities may be approached in terms of the one-electron energies

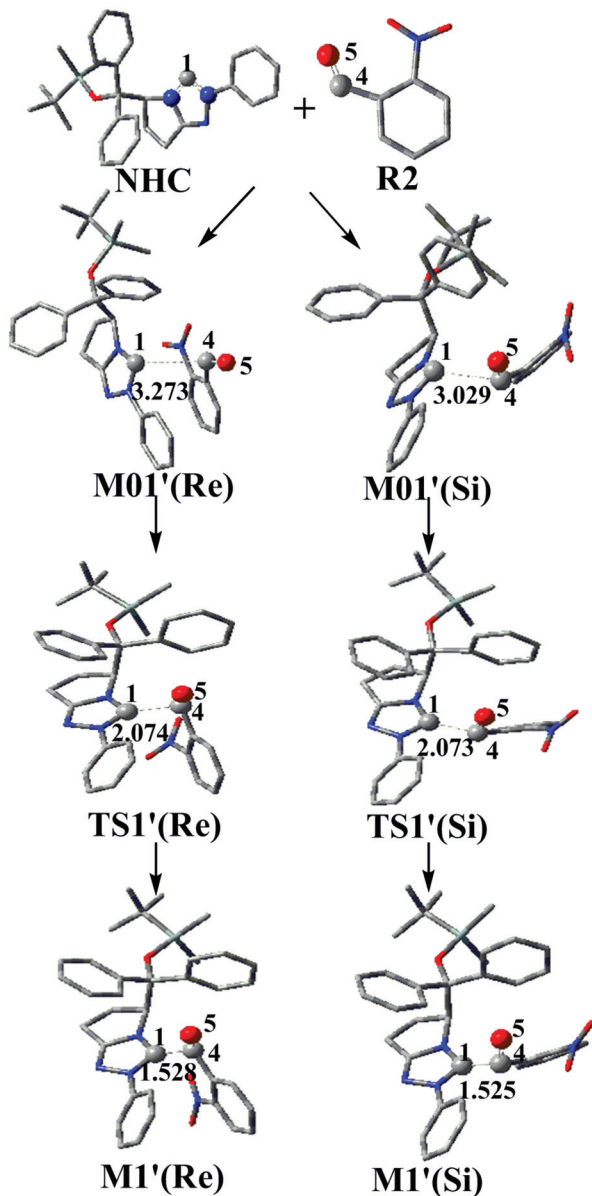
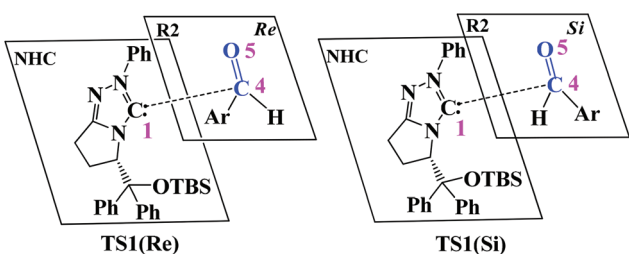


Fig. 5 Optimized structures of the reactants (NHC and R2), transition states  $\text{TS1}'(\text{Re}\&\text{Si})$ , and intermediates  $\text{M1}'(\text{Re}\&\text{Si})$  (distances in Å).



Scheme 6 The two attack modes of NHC to R2 via  $\text{TS1}'(\text{Re}\&\text{Si})$ .

of the frontier molecular orbital HOMO and LUMO,  $E_{\text{H}}$  and  $E_{\text{L}}$ , as  $\mu \approx (E_{\text{H}} + E_{\text{L}})/2$  and  $\eta \approx (E_{\text{L}} - E_{\text{H}})$ . Moreover, according the HOMO energies obtained within the Kohn-Sham scheme,<sup>20b,c</sup>

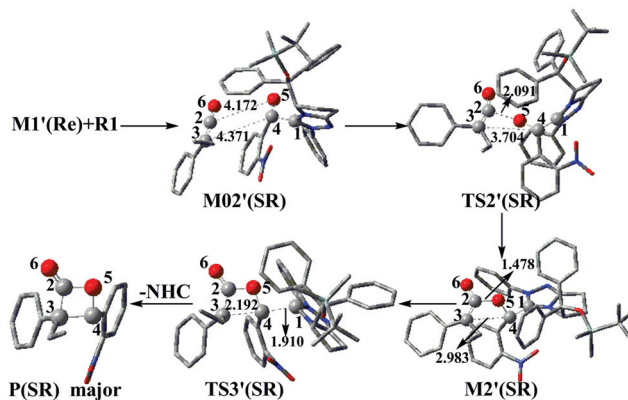


Fig. 6 Optimized structures for  $\text{M02}'(\text{SR})$ ,  $\text{TS2}'(\text{SR})$ ,  $\text{M2}'(\text{SR})$ ,  $\text{TS3}'(\text{SR})$ , and  $\text{P}(\text{SR})$  (distances in Å).

Table 3 Energy of HOMO ( $E_{\text{H}}$ , in a.u.), energy of LUMO ( $E_{\text{L}}$ , in a.u.), electronic chemical potential ( $\mu$ , in a.u.), chemical hardness ( $\eta$ , in a.u.), global electrophilicity ( $\omega$ , in eV) and global nucleophilicity ( $N$ , in eV) of some reactants (SR) involved in the [2 + 2] cycloaddition step

SR	$E_{\text{H}}$ (a.u.)	$E_{\text{L}}$ (a.u.)	$\mu$ (a.u.)	$\eta$ (a.u.)	$\omega$ (eV)	$N$ (eV)	$S$
R1	-0.261	-0.0028	-0.131	0.258	0.898	3.510	1.938
R2	-0.345	-0.081	-0.213	0.264	2.340	1.224	1.894
M1(E)	-0.214	-0.014	-0.114	0.200	0.871	4.789	2.500
M1(Z)	-0.215	-0.020	-0.118	0.195	0.972	4.762	2.564

Domingo and co-workers gave the nucleophilicity index  $N$  to handle a nucleophilicity scale.<sup>21</sup> The nucleophilicity index is defined as  $N = E_{\text{HOMO}(\text{SR})} - E_{\text{HOMO}(\text{TCE})}$ . This nucleophilicity scale is referenced to tetracyanoethylene (TCE). Following the definition of these indices, in this reaction (Table 3), R2 is classified as the electrophile ( $\omega = 2.340$  eV). R1, M1(E), M1(Z) are the nucleophiles with the values of 3.510, 4.789, and 4.762 eV, respectively. The nucleophile values of M1(E), M1(Z) are obviously larger than R1, indicating that coordination of NHC to the ketene carbon atom of R1 noticeably strengthens the nucleophilicity of R1, and thus promotes the [2 + 2] cycloaddition between R1 and R2.

Generally, the condensed-to-atom Fukui functions ( $f_k$ ) at the atom  $k$  can be evaluated from differences in atomic charges:  $f_k^+ = q_k(N) - q_k(N+1)$ ,  $f_k^- = q_k(N-1) - q_k(N)$ , and  $f_k^0 = 0.5[q_k(N-1) - q_k(N+1)]$ , where  $q_k$  is the electronic charge of atom  $k$  and  $N$  is the number of electrons. The three condensed Fukui functions characterize the reactivity preferences for nucleophilic, electrophilic, and radical attacks, respectively.<sup>22</sup> The global softness is expressed as  $S = 1/2\eta$ , and the corresponding condensed-to-atom softnesses are  $s_k^+ = f_k^+S$ ,  $s_k^- = f_k^-S$ , and  $s_k^0 = f_k^0S$ , which are suited for studies of nucleophilic, electrophilic, and radical attacks, respectively.<sup>23</sup> As shown in Table 4, we have calculated the Fukui functions and local softnesses for the reacting atoms C2 and C3 at the different conditions, and it is easily found that both the nucleophilicity and electrophilicity of C3 atom are strengthened under the NHC-catalyzed conditions, which should be helpful to promote the reaction to occur.

**Table 4** The condensed-to-atom Fukui functions and local softnesses of the reacting atoms C2 and C3 under the non-catalyzed and NHC-catalyzed conditions

SR	$f_{C2}^+$	$f_{C2}^-$	$f_{C3}^+$	$f_{C3}^-$	$S_{C2}^+$	$S_{C2}^-$	$S_{C3}^+$	$S_{C3}^-$
R1	0.693	0.118	-0.245	0.212	1.343	0.229	0.475	0.411
M1(E)	0.030	0.011	0.043	0.319	0.075	0.028	0.108	0.798
M1(Z)	0.037	0.021	0.037	0.275	0.095	0.054	0.095	0.705

## 4. Conclusions

In this paper, the detailed mechanisms and stereoselectivities for the NHC-catalyzed ketene and aldehyde [2 + 2] cycloaddition reaction have been investigated using density functional theory (DFT). We have suggested and studied two possible reaction mechanisms (mechanisms A and B) of the NHC-catalyzed ketene [2 + 2] cycloaddition reaction to generate four kinds of stereoisomer at the M062X/6-31G(d,p) level in toluene solvent using the IEF-PCM model. The calculated results reveal that the favorable mechanism (mechanism A) involves three steps: initially **NHC** approaches the carbonyl group of the ketene to form an intermediate **M1(E&Z)**. The second step is a [2 + 2] cycloaddition process, which can lead to four kinds of intermediate *via* different diastereotopic transition states. The remaining step involves the dissociation of catalyst **NHC** and the product. Moreover, the [2 + 2] cycloaddition step is calculated to be both the rate-determining and stereoselectivity-determining step, and the energy barriers of 15.88, 19.68, 13.58 and 17.07 kcal mol<sup>-1</sup> correspond to the stereoisomer transition states **TS2(SS,RR,SR&RS)**, respectively. The energetic favorability of the *SR* configuration stereoisomer suggests that it should be the dominant product, which is in good agreement with the experiment. That is to say, the transition state associated with the second step should be the key for the stereoselectivity of the title reaction. Furthermore, analysis of global and local reactivity indexes has been performed to explain the role of catalyst NHC. In summary, this study provides a theoretical model for predicting the stereoselectivity of the product, which should be helpful for rational design of potent catalysts to synthesize  $\beta$ -lactones with high stereoselectivity.

## Acknowledgements

The work described in this paper was supported by the National Natural Science Foundation of China (no. 21303167 and J1210060) and China Postdoctoral Science Foundation (no. 2013M530340).

## References

- (a) Z. Wan and S. G. Nelson, *J. Am. Chem. Soc.*, 2000, **122**, 10470; (b) J. Douglas, J. E. Taylor, G. Churchill, A. M. Z. Slawin and A. D. Smith, *J. Org. Chem.*, 2013, **78**,

- 3925; (c) H. Abe, I. Matsubara and Y. Doi, *Macromolecules*, 1995, **28**, 844.
- 2 (a) T. T. Tidwell, *Eur. J. Org. Chem.*, 2006, 563; (b) S. G. Nelson, W. S. Cheung, A. J. Kassick and M. A. Hilfiker, *J. Am. Chem. Soc.*, 2002, **124**, 13654.
- 3 (a) C. Schneider, *Angew. Chem., Int. Ed.*, 2002, **41**, 744; (b) H. W. Yang and D. Romo, *Tetrahedron*, 1999, **55**, 6403; (c) Y. C. Wang, R. L. Tennyson and D. Romo, *Heterocycles*, 2004, **54**, 605.
- 4 (a) S. G. Nelson, B. K. Kim and T. J. Peelen, *J. Am. Chem. Soc.*, 2000, **122**, 9318; (b) C. M. Rasik and M. K. Brown, *J. Am. Chem. Soc.*, 2013, **135**, 1673; (c) P. Meier, F. Broghammer, K. Latendorf, G. Rauhut and R. Peters, *Molecules*, 2012, **17**, 7121; (d) S. Chidara and Y. M. Lin, *Synlett*, 2009, 1675.
- 5 A. B. Concepcion, K. Maruoka and H. Yamamoto, *Tetrahedron*, 1995, **51**, 4011.
- 6 L. He, H. Lv, Y. R. Zhang and S. Ye, *J. Org. Chem.*, 2008, **73**, 8101.
- 7 (a) J. M. Pons, A. Pommier and M. Rajzmann, *J. Mol. Struct. (THEOCHEM)*, 1991, **119**, 361; (b) B. Lecea, A. Arrieta, G. Roa, J. M. Ugalde and F. P. Cossio, *J. Am. Chem. Soc.*, 1994, **116**, 9613; (c) B. Lecea, A. Arrieta, X. Lopez, J. M. Ugalde and F. P. Cossio, *J. Am. Chem. Soc.*, 1995, **117**, 12314; (d) S. Yamabe, K. Kuwata and T. Minato, *Theor. Chem. Acc.*, 1999, **102**, 139; (e) J. M. Pons, M. Oblin, A. Pommier, M. Rajzmann and D. Liotard, *J. Am. Chem. Soc.*, 1997, **119**, 3333.
- 8 D. H. Wei, W. J. Zhang, Y. Y. Zhu and M. S. Tang, *J. Mol. Catal. A: Chem.*, 2010, **326**, 41.
- 9 (a) D. H. Wei, Y. Y. Zhu, C. Zhang, D. Z. Sun, W. J. Zhang and M. S. Tang, *J. Mol. Catal. A: Chem.*, 2011, **334**, 108; (b) Y. Qiao and K. L. Han, *Org. Biomol. Chem.*, 2012, **10**, 7689; (c) W. J. Zhang, D. H. Wei and M. S. Tang, *J. Org. Chem.*, 2013, **78**, 11849; (d) Y. X. Liu, D. J. Zhang, S. W. Bi and C. B. Liu, *Org. Biomol. Chem.*, 2013, **11**, 336; (e) J. N. Gibb and M. G. Jonathan, *Org. Biomol. Chem.*, 2013, **11**, 90; (f) Z. Y. Li, D. H. Wei, Y. Wang, Y. Y. Zhu and M. S. Tang, *J. Org. Chem.*, 2014, **79**, 3069.
- 10 M. J. T. Frisch, et al., *GAUSSIAN 09 (Revision C.01)*, Gaussian, Inc., Wallingford, CT, 2010.
- 11 (a) D. H. Wei, L. Fang, M. S. Tang and C. G. Zhan, *J. Phys. Chem. B*, 2013, **117**, 13418; (b) R. Lee, F. R. Zhong, B. Zheng, Y. Z. Meng, Y. X. Lu and K. W. Huang, *Org. Biomol. Chem.*, 2013, **11**, 4818; (c) M. M. Vallejos, N. M. Peruchena and S. C. Pellegrinet, *Org. Biomol. Chem.*, 2013, **11**, 7953; (d) D. H. Wei, X. Q. Huang, J. J. Liu,

- M. S. Tang and C. G. Zhan, *Biochemistry*, 2013, **52**, 5145;  
 (e) D. H. Wei, B. L. Lei, M. S. Tang and C. G. Zhan, *J. Am. Chem. Soc.*, 2012, **134**, 10436; (f) W. J. Zhang, Y. Y. Zhu, D. H. Wei and M. S. Tang, *J. Comput. Chem.*, 2012, **33**, 715;  
 (g) D. H. Wei and M. S. Tang, *J. Phys. Chem. A*, 2009, **113**, 11035.
- 12 E. H. Krenske, *Org. Biomol. Chem.*, 2013, **11**, 5226.
- 13 (a) Y. Zhao and D. G. Truhlar, *Theor. Chem. Acc.*, 2008, **120**, 215; (b) Y. Zhao and D. G. Truhlar, *Acc. Chem. Res.*, 2008, **41**, 157; (c) Y. Zhao and D. G. Truhlar, *J. Chem. Theory Comput.*, 2008, **4**, 1849.
- 14 (a) V. Barone and M. Cossi, *J. Phys. Chem. A*, 1998, **102**, 1995; (b) B. Mennucci and J. Tomasi, *J. Chem. Phys.*, 1997, **106**, 5151.
- 15 (a) C. Gonzalez and H. B. Schlegel, *J. Chem. Phys.*, 1989, **90**, 2154; (b) C. Gonzalez and H. B. Schlegel, *J. Phys. Chem.*, 1990, **94**, 5523.
- 16 (a) L. Sun, M. S. Tang, H. M. Wang, D. H. Wei and L. L. Liu, *Tetrahedron: Asymmetry*, 2008, **19**, 779; (b) D. H. Wei, M. S. Tang, J. Zhao, L. Sun, W. J. Zhang, C. Zhao, S. R. Zhang and H. M. Wang, *Tetrahedron: Asymmetry*, 2009, **20**, 1020.
- 17 F. P. Cossio, A. Arrieta and M. A. Sierra, *Acc. Chem. Res.*, 2008, **41**, 925.
- 18 W. J. Zhang, Y. Y. Zhu, D. H. Wei, Y. X. Li and M. S. Tang, *J. Org. Chem.*, 2012, **77**, 10729.
- 19 (a) L. R. Domingo and P. Perez, *Org. Biomol. Chem.*, 2013, **11**, 4350; (b) R. G. Parr and R. G. Pearson, *J. Am. Chem. Soc.*, 1983, **105**, 7512.
- 20 (a) L. R. Domingo, J. A. Saez, R. J. Zaragoza and M. Arno, *J. Org. Chem.*, 2008, **73**, 8791; (b) L. R. Domingo, M. T. Picher and J. A. Saez, *J. Org. Chem.*, 2009, **74**, 2726; (c) L. R. Domingo, M. J. Aurell, P. Perez and R. Contreras, *Tetrahedron*, 2002, **58**, 4417.
- 21 (a) W. Kohn and L. J. Sham, *Phys. Rev.*, 1965, **137**, A1697; (b) L. J. Sham and W. Kohn, *Phys. Rev.*, 1966, **145**, 561; (c) L. R. Domingo, E. Chamorro and P. Perez, *J. Phys. Chem. A*, 2008, **112**, 4046; (d) L. R. Domingo, P. Perez and J. A. Saez, *RSC Adv.*, 2013, **3**, 1486; (e) E. Chamorro, P. Perez and L. R. Domingo, *Chem. Phys. Lett.*, 2013, **582**, 141.
- 22 (a) P. P. Zhou, P. W. Ayers, S. B. Liu and T. L. Li, *Phys. Chem. Chem. Phys.*, 2012, **14**, 9890; (b) W. T. Yang and W. J. Mortier, *J. Am. Chem. Soc.*, 1986, **108**, 5708; (c) R. G. Parr and W. T. Yang, *J. Am. Chem. Soc.*, 1984, **106**, 4049.
- 23 R. K. Roy, S. Krishnamurti, P. Geerlings and S. Pal, *J. Phys. Chem. A*, 1998, **102**, 3746.